

HYDRAULICS

INVESTIGATION OF HELICOIDAL FLOW IN RIFLED PIPELINES FOR SLURRY TRANSPORT*

by

I. V. NAGY and M. DULOVICS-DOMBI

Institute of Water Management and Hydraulic Engineering, Technical University, Budapest

(Received February 8, 1972)

Introduction

The hydraulic behaviour of pressure flow in pipes is one of the classical and perhaps most comprehensively investigated phenomena of fluid mechanics. On the other hand, laws governing two-phase flow, i.e. the flow of a mixture of water and another substance are known approximately only. The flow field is becoming increasingly intricate in case of a rifled pipe, shown in Fig. 1, giving rise to a constraint for helicoidal flow. In course of the experiments described below, hydraulic features of this induced helicoidal flow are examined by using both clear water and slurry.

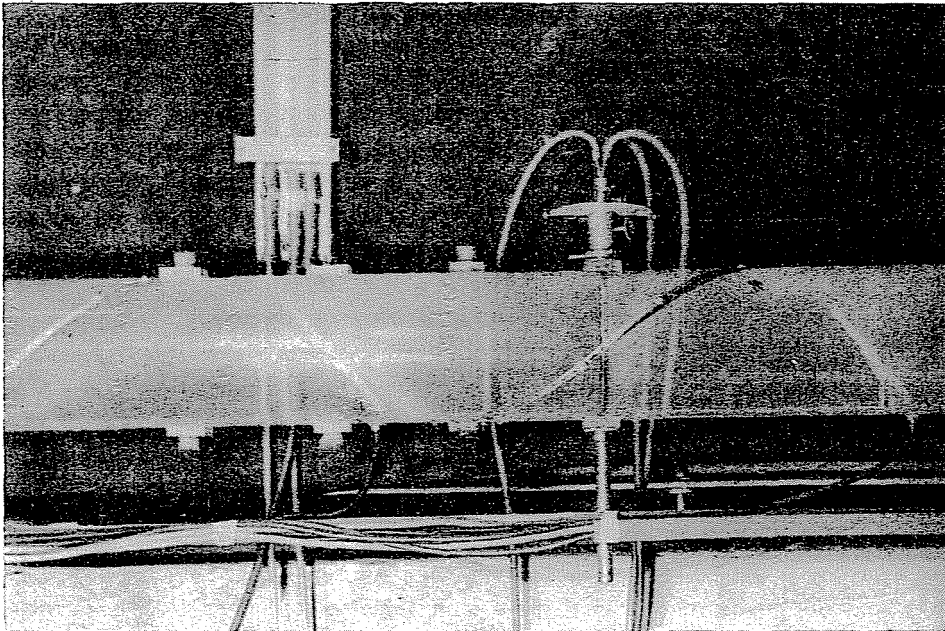


Fig. 1. Test pipe

* Research sponsored by the National Water Authority.

Review of the literature

The first references to the theory of helicoidal flow in pipes are found in the works of GROMEKA [2] and then of MILOVITCH [3]. The said authors made their departure from the hypothesis of a homogeneous helicoidal flow, with a velocity distribution in the main direction of flow being given. It was proved by ПОТАПОВ and ПИШКИН [4] that transversal velocity components are to be calculated independently of the one in the main direction of flow.

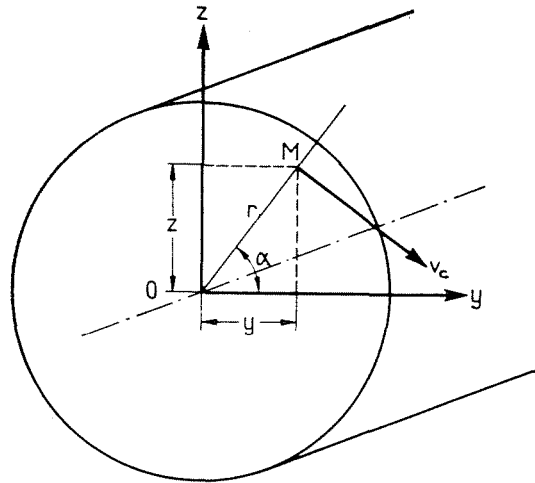


Fig. 2. Notations used in analysis

The basic equation of helicoidal flow may be written as follows [4]:

$$\frac{\partial^2 \psi}{\partial y^2} + \frac{\partial^2 \psi}{\partial z^2} + k^2 \psi = 0. \quad (1)$$

By introducing the cylindrical co-ordinates of Fig. 2 and using the substitutions

$$y = r \cos \alpha, \quad z = r \sin \alpha$$

one arrives to

$$\frac{\partial^2 \psi}{\partial r^2} + \frac{1}{r} \frac{\partial \psi}{\partial r} + \frac{1}{r^2} \frac{\partial^2 \psi}{\partial \alpha^2} + k^2 \psi = 0.$$

By supposing the flow to be symmetrical to the axis OX , or in other terms, by assuming the validity of the equation

$$\frac{\partial \psi}{\partial \alpha} = 0$$

one may write:

$$\frac{\partial^2 \psi}{\partial r^2} + \frac{1}{r} \frac{\partial \psi}{\partial r} + k^2 \psi = 0. \tag{2}$$

Again, by introducing the new variable

$$\omega = kr \tag{3}$$

Eq. 2 becomes one of the Bessel type:

$$\frac{\partial^2 \psi}{\partial \omega^2} + \frac{1}{\omega} \frac{\partial \psi}{\partial \omega} + \psi = 0. \tag{4}$$

The solution of this differential equation is yielded by a first-degree Bessel function of zero order, i.e.:

$$\psi = CI_0(\omega) = CI_0(kr). \tag{5}$$

The velocity of circulation at a distance r from the pipe axis will be

$$v_c = \frac{\partial \psi}{\partial r} = -CkI_1(kr) \tag{6}$$

with I_1 being a first-degree Bessel function of the first order, related to I_0 according to the equation

$$\frac{dI_0(\omega)}{d\omega} = -I_1(\omega). \tag{7}$$

Components of the transversal velocity, parallel to the axes OY and OZ , respectively, are:

$$v = v_c \frac{z}{r}; \quad w = -v_c \frac{y}{r}.$$

Rotational velocity components of the angular velocity parallel to the axis OX depend solely upon characteristics of the helicoidal flow prevailing in certain planes of cross section. Thus, Eqs (6) and (4) will lead to

$$\zeta = \frac{1}{2} \frac{\partial v_c}{\partial r} + \frac{v_c}{r} = -\frac{k^2}{2} \psi = -\frac{Ck^2}{2} I_0(kr). \tag{8}$$

For $\omega = 0$, $I_0(0) = 1$ and $I_1(0) = 0$ and hence in the pipe axis ($r = 0$) one will have

$$\psi = C; \quad v_c = 0; \quad \zeta = -Ck^2/2. \quad (9)$$

In order to illustrate variations of the factors ψ , v_c and ζ along the pipe radius, Fig. 3 shows curves of the functions $I_0(\omega)$ and $I_1(\omega)$ to be constructed by means of tables of Bessel functions. Ordinates of the curve I_0 are proportional to values of either ψ or ζ whilst ordinates of the curve I_1 are proportional to values of v_c .

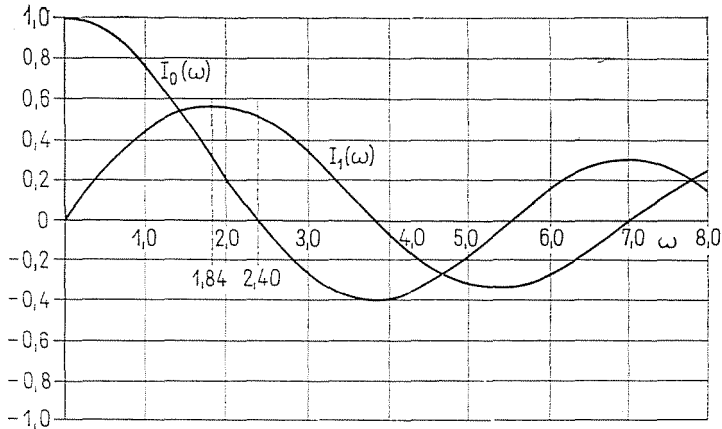


Fig. 3. Plots of Bessel functions

From the now described theoretical considerations it follows that in case of an induced helicoidal flow, one of the two hypotheses below may become accepted:

1. the velocity v_c assumes its maximum value at the pipe wall;
2. the angular velocity ζ (and hence, the stream function ψ) is equalling zero at the pipe wall.

In case of a rectangular pipe, the above two conditions will coincide but for any curvilinear profile they are mutually exclusive.

As to be seen from Fig. 3 showing the Bessel functions, the function $I_1(\omega)$ attains its maximum at $\omega = kR = 1.84$ or $k = 1.84/R$, with R being the pipe radius, and hence, $I_1(1.84) = 0.582$. The function $I_0(\omega)$ becomes zero at $\omega = 2.40$ or $k = 2.40/R$, where $I_1(2.40) = 0.519$.

In order to facilitate further calculations and the evaluation of test results it is expedient to express the values C , ψ and v_c by means of the rotational velocity v_0 at the pipe wall by aid of Eq. (6) yielding in the first case ($r = R$):

$$C = -0.93 v_0 R \quad (10)$$

$$\psi = -0.93 v_0 R I_0(1.84 r/R) \tag{11}$$

$$v_c = 1.71 v_0 I_1(1.84 r/R) \tag{12}$$

and in the second case

$$C = -0.803 v_0 R \tag{13}$$

$$\psi = -0.803 v_0 R I_0(2.40 r/R) \tag{14}$$

$$v_c = 1.926 v_0 I_1(2.40 r/R) \tag{15}$$

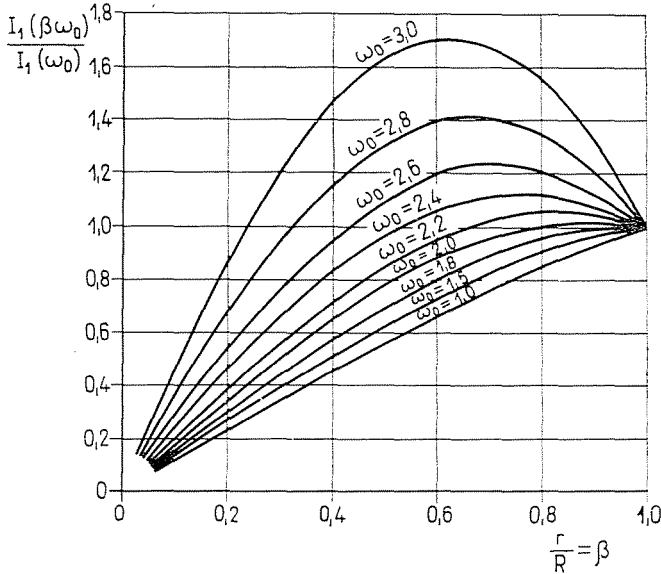


Fig. 4. Ratios of Bessel functions

Consequently, the problem consists in measuring some values of the rotational velocity v_c along the pipe radius in order to determine the parameters k and C . Let the measurements be performed at points $r = \beta R$ and $r = R$. Then, according to Eq. (6), one may write:

$$v = CkI_1(\beta, \omega_0) ; \quad v_1 = CkI_1(\omega_0)$$

where $\omega = kr$ and $\omega_0 = kR$. The ratio of these two velocities may be written as:

$$\frac{v_\beta}{v_1} = \frac{I_1(\beta, \omega_0)}{I_1(\omega_0)} = f(\beta, \omega_0)$$

with v_1 denoting rotational velocity at the pipe wall. The function $f(\beta, \omega_0)$ is shown in Fig. 4, to be used directly to the determination of values of k and C in the knowledge of measured values of rotational velocity.

Research apparatus and procedures

The experiments were performed in a plastic tube, using a closed system of recirculation. The tube had a diameter of 0.15 m and a length of 10.25 m. The circulating discharge was made variable by means of the pump-driving motor, equipped with a variable-ratio transmission.

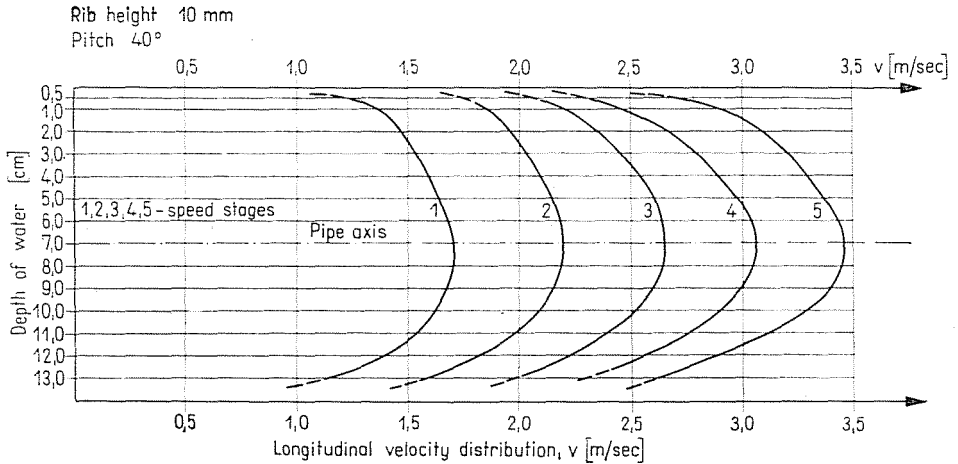


Fig. 5. Longitudinal velocity distribution. 1, 2, 3, 4, 5 — speed stages of pumps and motor

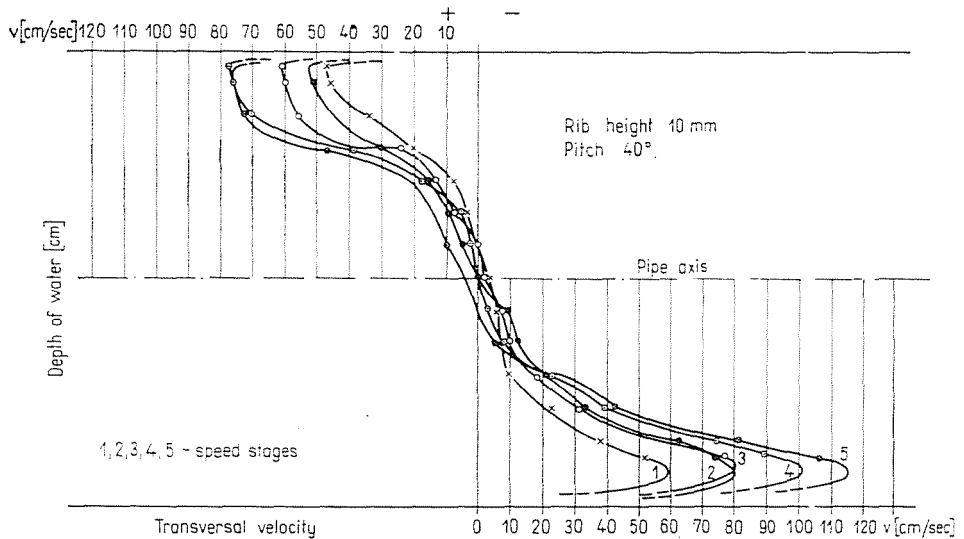


Fig. 6. Transversal velocity. 1, 2, 3, 4, 5 — speed stages of pump and motor

Experiments were made by using different kinds of rifling, having the following characteristics:

1. pitch 40°, with ribs 10 mm high and 5 mm wide;

2. pitch 40°, with ribs 5 mm high and 5 mm wide;
3. pitch 30°, with ribs 5 mm high and 5 mm wide.

Measurements, using clear water, were made in several cross sections. Longitudinal and transversal velocity distributions in one of the cross sections, pertaining to 5 different discharges, are shown in Figs 5 and 6.

During the *second stage* of experiments, sediment consisting of river sand with an average diam. $d = 0.33$ mm and of silt with $d = 0.025$ mm was added to water in concentrations of 3, 4, 5, 6, 8, 10, 12.5, 15, 20, 25, 30 and 55 per cent by weight, using also varying discharges.

In case of a plain pipe, the distribution of concentration along the depth is characterized by the well-known curve of Fig. 7. The same feature for rifled pipe is shown in Fig. 8, differing entirely from the previous one.

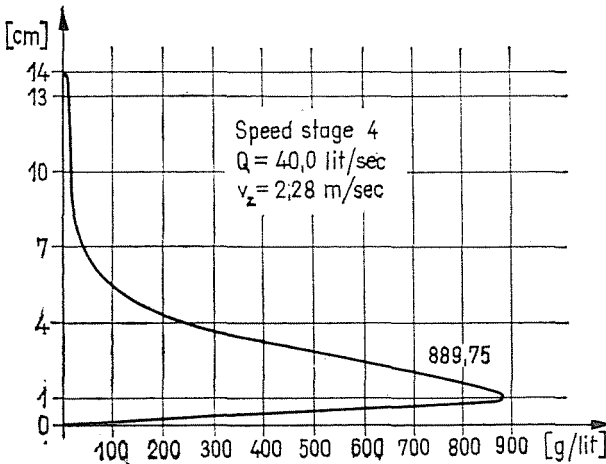


Fig. 7. Distribution of concentration within the pipe

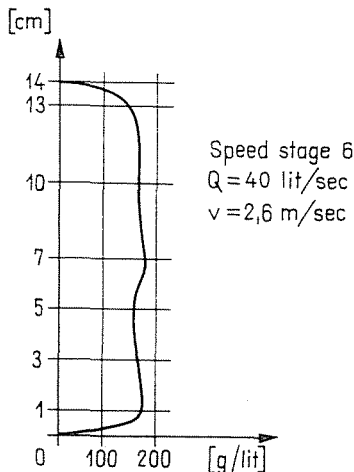


Fig. 8. Distribution of concentration within the pipe

Analysis of data and discussion of results

When analysing test results, the following two questions had to be answered:

1. Distribution of transversal velocities, essential from the point of transporting and keeping in suspension the sediments.

2. Dependence of the friction factor (hydraulic loss) upon type of rifling and changes in concentration.

Calculation of rotational velocities

According to Fig. 6, the rotational velocity at a distance of $0.5r$ from the pipe axis is $v_{0.5} = 30$ cm/sec for the second speed stage, whilst its maximum at the pipe wall is $v_1 = 52$ cm/sec. The function $f(\beta, \omega_0)$ will thus assume the value

$$f(\beta, \omega_0) = \frac{30}{52} = 0.57.$$

In Fig. 4, $r/R = \beta = 0.5$ and $f(\beta, \omega) = 0.57$ will yield the interpolated value of $\omega_0 = 1.1$ or $k = 1.1/R$. Hence, involving Fig. 2 and Eq. (6), for the pipe circumference one may write:

$$52 = C \frac{1.1}{R} I_1(1.1) = 1.1 \times 0.43 C/R = 0.473 C/R$$

yielding

$$C = 52R/0.473 = 105R.$$

Accordingly, the radial distribution of v_c is described by

$$v_c = 105R \frac{1.1}{R} I_1(1.1 r/R) = 115.5 I_1(1.1 r/R)$$

resulting in $v_c = 0.473 \times 115.5 = 54.6$ cm/sec in the vicinity of the pipe wall. The relationship $r/R = f(v_c)$ is shown in Fig. 9.

Velocity measurements and calculations permit us to draw the following conclusions:

— the shape of the curve of longitudinal velocity distribution is similar to that occurring in smooth pipes, but becomes more and more distorted with an increasing average velocity: the difference between mean velocity and the maximum velocity in the pipe axis is growing;

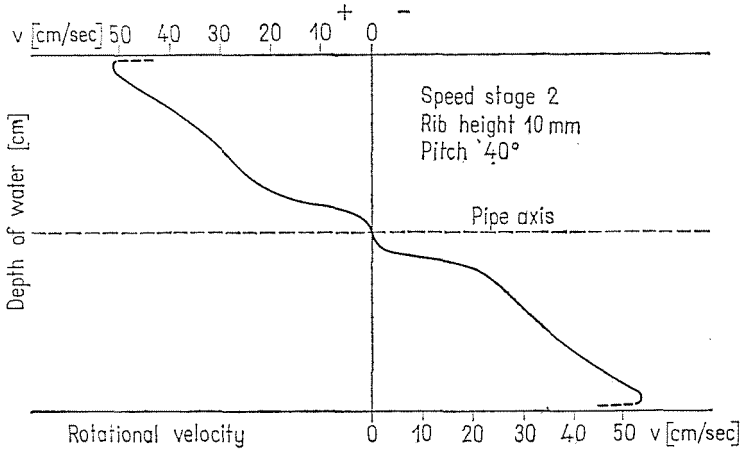


Fig. 9. Distribution of the rotation velocity within the pipe

— transversal velocity components assume a zero value in the pipe axis and the diameter of the irrotational zone is decreasing with increasing mean velocity;

— as seen from the figure of resulting rotational velocities, helicoidal rifling has a transforming effect upon the velocity distribution of the smooth pipe and thus, the same amount of energy has a sediment transport capacity several times of that before.

Investigations into sediment transport capacity and resistances

As seen from Figs 7 and 8, sediment transport is almost uniformly distributed over the whole pipe cross section, owing to the presence of rifling.

The beginning of deposit formation at the lower part of the pipe is linked with a much lower mean velocity in rifled pipes than in smooth ones. For instance, continuous depositing took place at $v_m = 1.60$ m/sec for a concentration of 10 per cent by weight in the plain pipe whereas in a rifled pipe, deposits have occurred spotwise only at velocities of 0.9 to 1.0 m/sec.

Hydraulic losses

Losses occurring during slurry movement have been calculated upon basis of the modified Darcy — Weisbach formula, to be written as

$$h_v = [f_w + f_1(v, c) + f_2(v, c)] \frac{l}{d} \frac{v^2}{2g}$$

where f_w — friction factor for plain pipe and clear water;

f_1 and f_2 — friction factors owing to sediment and to rifling, respectively.

According to our experiments, both depend on flow velocity v and slurry concentration c ;

l and d — pipe length and diameter, respectively;

g — gravity constant.

When plotting the pressure gradient $\Delta h/\Delta l$ against the flow velocity v one sees (Fig. 10) that in case of plain pipes

— the above relationship for zero concentration (clear water) is represented by a straight line;

— increasing sediment concentration involves an increase of losses too, but this rise is considerable only up to about 1.5 to 2.5 m/sec of flow velocity.

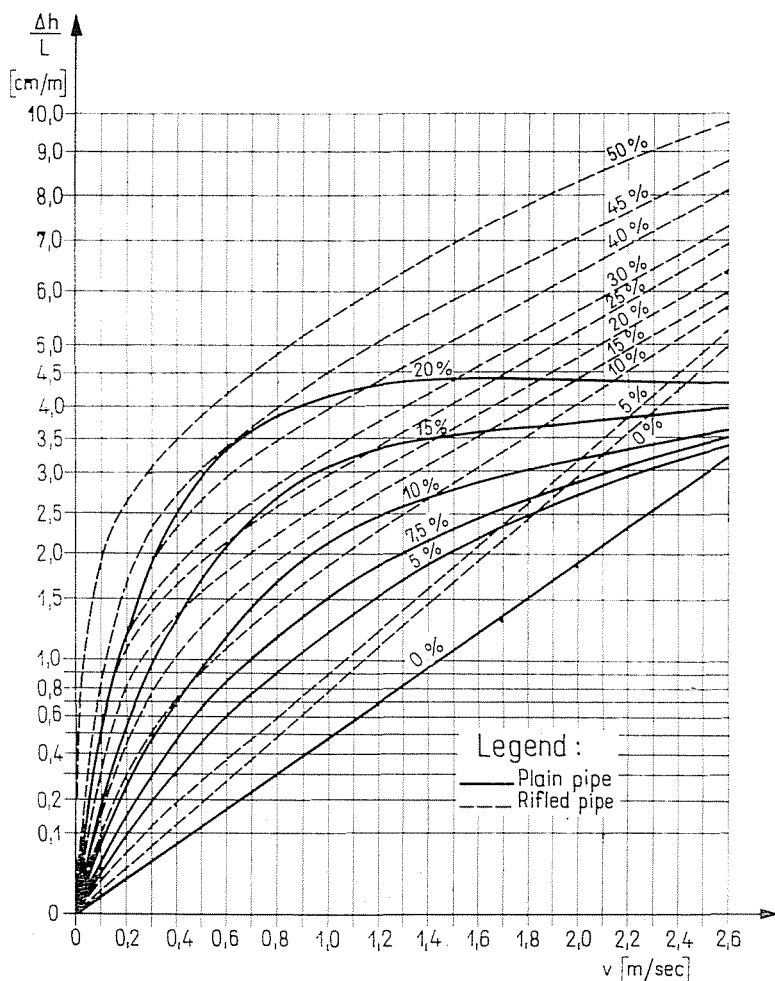


Fig. 10. Specific head loss vs. transport velocity

Further upwards, in the range of pure turbulence, losses are less depending upon flow velocity. This phenomenon may indicate that with an increasing concentration the intensity of turbulence decreases and hence, there is a relatively lower value of internal friction.

In case of rifled pipes (exemplified by the one with a pitch of 40° and ribs 0.5 × 0.5 cm), losses vs. velocity also are presented by a straight line for clear water (Fig. 11). At low velocities, losses are rapidly increasing with concentration. But it seems that curves of losses pertaining to various concentrations are approaching the straight line of clear water and these curves form

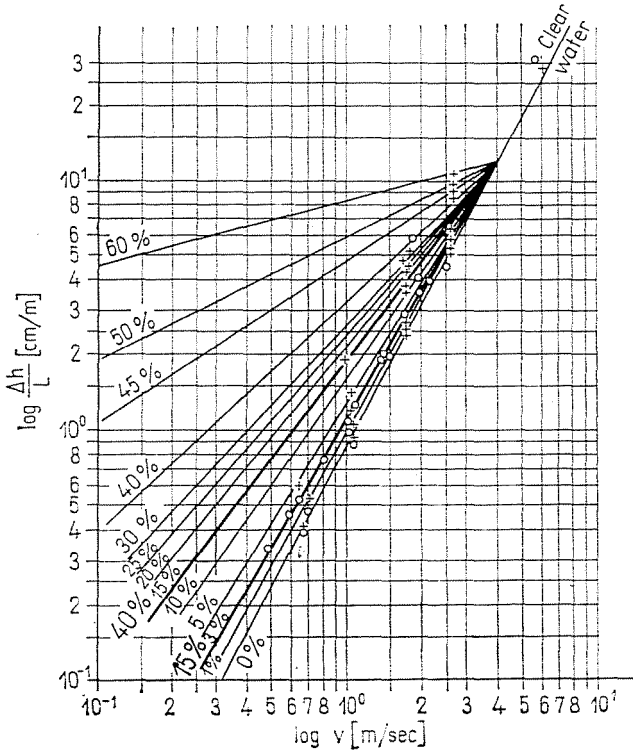


Fig. 11. Specific loss vs. transport velocity, 40° pitch, 5 × 5 cm ribs.
 Legend: + rivers and, O silt

arrays with different origins for various types of rifling. The slopes of the straight lines decrease with increasing concentration, leading to the following conclusions:

- the increase of concentration is accompanied by a less and less increasing hydraulic loss up to a certain velocity limit only (4.0 m/sec in the example);
- the equalization of the turbulent velocity field are manifest by the fact that the diameter, energy content and propagation velocity of secondary turbulent formations giving rise to internal friction are decreasing substantially

(or, in other terms, the structure of the turbulent velocity field becomes refined) entailing the decrease of mean pulsation components.

As a final conclusion it may be stated that the *degree of turbulence intensity of the basic turbulent flow is inversely proportional to changes in concentration* if a constant mean velocity is assumed.

One also arrives to similar results if at a constant transport velocity, the specific energy loss vs. slurry concentration relationship is plotted (Fig. 12). For the same type of rifling, curves pertaining to various velocities go over into an array of straight lines if plotted on semi-logarithmic paper. Upon base

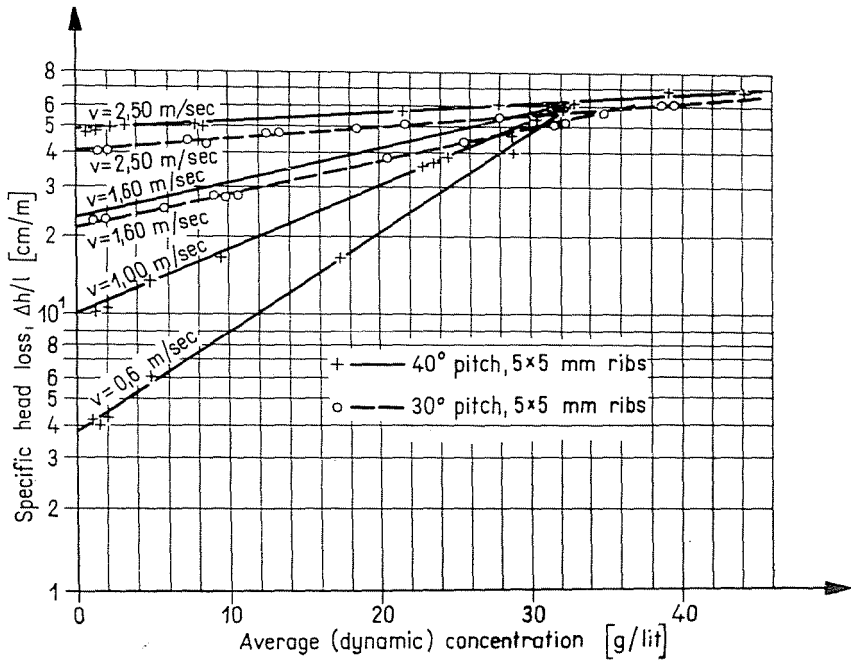


Fig. 12. Slurry concentration

of these straight lines it is possible to select the *economic transport velocity* pertaining to given values of slurry concentration.

Finally, the relationship of overall friction factor vs. Reynolds number is shown in Fig. 13. This consists of two parts, similarly to those determined by NIKARUDSE. When applying clear water and using a log-log paper, straight lines of the rifled pipes are parallel to the corresponding lines of plain pipes. In case of a slurry transport, however, the straight lines of rifled pipes are approaching the straight line of the plain pipe beyond a certain value of Re , forming thus an array.

The said break points lie within the range of Reynolds numbers 3 to 4×10^5 . This type of analysis refers again to the fact that there is no sub-

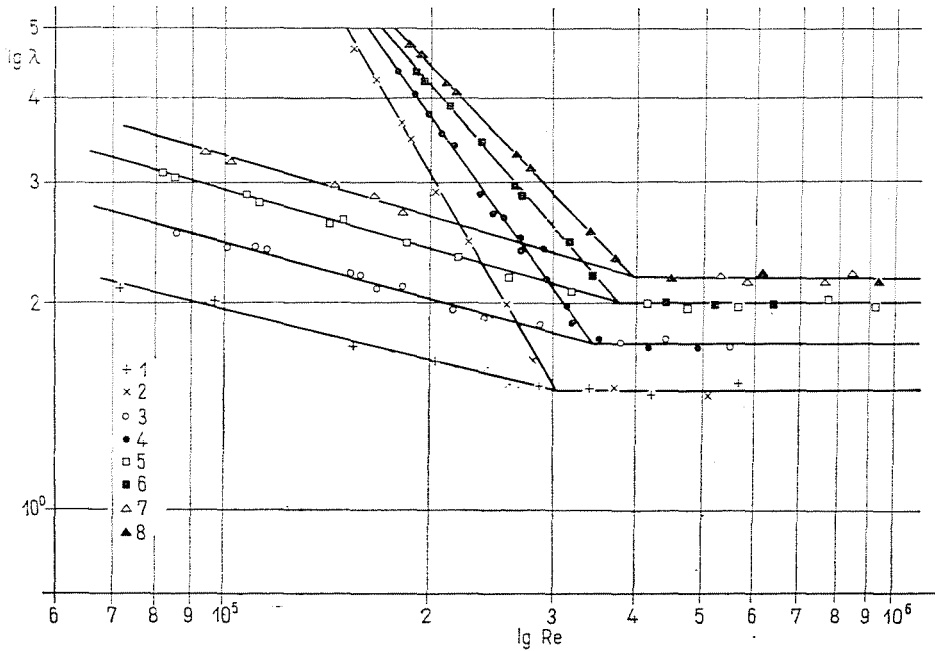


Fig. 13. Loss coefficient vs. Reynolds number; slurry concentration 50 per cent by weight. + — plain pipe, clear water. x — plain pipe, slurry. o — 30° pitch, clear water. ● — 30° pitch, slurry. □ — 40° pitch, 5×5 mm ribs, clear water. ■ — 40° pitch, 5×5 mm ribs, slurry. △ — 40° pitch, 10×5 mm ribs, clear water. ▲ — 40° pitch, 10×5 mm ribs, slurry

stantial difference between the losses occurring in a plain or a rifled pipe. Losses in a rifled pipe will even be lower than in a plain one, referred to the same rate of solid transport. Thus, the *energy consumption per unit weight of transported solids* will be much more favourable with the use of rifled pipes.

Summary

The paper has reviewed the hydraulic characteristics of induced helicoidal flow in pipes. Sets of measurements have been carried out in order to determine velocity distribution and pressure gradient of clear water. Experiments included plain pipes and various types of rifled pipes. In the course of slurry transport experiments, sediment concentration of sand and silt has been increased up to 50 per cent by weight. Measurements proved concentration distribution to become nearly uniform as an effect of rifling, accompanied by an equalization of the turbulent velocity field and a reduction of internal and wall friction. Energy requirement per unit weight of transported substance becomes thus reduced and consequently, the practical application of this method can be recommended.

References

1. SILBERMAN, E.: Effect of helix angle on flow in corrugated pipes. Journal of the Hydraulics Division of ASCE, Hy 11., Nov. 1970.
2. GROMEKA, I.: Some problems of incompressible fluid flow. (In Russian). Kazan, 1881.
3. MILOVITCH, A. Y.: Fundamentals of fluid flow. (In Russian). Moscow—Leningrad, 1933.
4. ПОТАПОВ, М. В.: Studies Vol. II. (In Russian). Moscow, 1951.

Prof. Dr. Imre V. NAGY, Director, } 1111 Budapest, Műegyetem rkp. 3,
 Senior Ass. Mrs. Maria DULOVICS-DOMBI } Hungary